M1 4/1*

Stochastic Response of Secondary Systems to Short-Duration Earthquakes

A. Der Kiureghian, T. Igusa

University of California, Dept. of Civil Engineering, Berkeley, California 94720, U.S.A.

Abstract

The response of secondary subsystems to short-duration excitation differs fundamentally from that of most structural systems. A method for nonstationary response analysis of general, linear, multiple-degree-of-freedom, multiply-supported secondary subsystems is presented. Through an example study, it is shown that, unlike ordinary structures, the peak response of secondary subsystems to short-duration earthquakes may occur long after termination of the excitation. Several essential characteristics of the response to short-duration seismic input are illustrated for the example secondary subsystem.

1. INTRODUCTION

Because of their composite nature, primary-secondary systems have four important dynamic characteristics which are uncommon among ordinary structures [10]: *Tuning* -- which is the coincidence of the frequencies of the primary and secondary subsystems; *Interaction* -- which is the feedback effect between motions of the two subsystems; *Non-Classical Damping* -- which occurs when the damping characteristics of the two subsystems are different, even when the subsystems are individually viscously and classically damped; and *Spatial Coupling* -- which is the effect of multiple support excitations of the secondary subsystem and is influenced by the locations of the support points and the stiffnesses of the connecting elements.

The above characteristics strongly affect the response of secondary subsystems to stochastic inputs. Tuning gives rise to closely spaced modes in the composite system whose responses to stochastic input are strongly correlated. The secondary response in each tuning mode is amplified and the correlation between these responses is usually negative. As a result, the neglect of this correlation results in gross overestimation (by hundreds of percent) of the secondary response [4]. Interaction reduces the response of the secondary subsystem, particularly for tuned systems where the ratio of secondary to primary masses is sufficiently large (i.e., greater than about 0.0001). Past studies based on cascaded systems [1, 6, 16] ignore the interaction effect and may grossly overestimate the true response. Tuning and interaction are also influential on the free-vibration response of the composite system. Due to the closely spaced modes and the feedback effect, the response of the system exhibits a beat phenomenon where the energy of the system is alternately exchanged between the primary and secondary subsystems. For an input excitation of short duration, this phenomenon may lead to peak responses of the secondary subsystem after termination of the excitation which are significantly greater than the peaks during the excitation [9, 15]. The non-classical damping of the composite system gives rise to complex-valued mode shapes, for which commonly used modal superposition methods are not directly applicable. Finally, for multiply supported secondary subsystems there is significant correlation between the motions at various support points. In current applications using cascaded systems [1] this correlation is not handled properly and is the source for significant errors.

In recent works [10, 11], the authors have formulated an efficient method for analysis of secondary subsystems which accurately accounts for the above four dynamic characteristics. The method consists of two steps: (a) synthesis of the modal properties of the composite primary-secondary system in terms of the known properties of the individual subsystems, and (b) dynamic response analysis by modal superposition employing the derived properties of the composite system. With this approach, closed-form solutions for the modal properties of the composite system are obtained through the use of perturbation theory and numerical solution of the eigenvalue problem for the composite system is avoided. The effects of interaction, tuning, non-classical damping, and spatial coupling are implicitly included in the derived modal properties. Furthermore, the effects of closely spaced modes, resulting from tuning, and the non-classical damping are explicitly accounted for in the response analysis. Methods for such analyses for stationary and nonstationary inputs, and for inputs described in terms of the response spectrum method, are presented in Refs. 8, 9 and 12.

In this paper, expressions for the root-mean-square and peak response of composite primary-secondary systems to stochastic inputs are presented. These results are applied to an example system to illustrate the important characteristics of the response of the secondary subsystem to short-duration earthquakes.

2. Response to Nonstationary Input

Expressions for the complex modal properties of composite primary-secondary systems are presented in Ref. 10. These expressions are in terms of the modal properties of the individual fixed-base subsystems and are either in closed-form or in terms of small eigenvalue problems. Once these properties are determined, the response of the system to stochastic input can be obtained through any modal superposition method that accounts for closely spaced modes and non-classical damping.

It is shown in Ref. 12 that the response of a linear, non-classically damped system in general can be expressed in terms of its modal contributions

$$v(t) = \sum_i [a_i h_i(t) + c\,\dot{h}_i(t)] \tag{1}$$

where $h_i(t)$ is the Duhamel integral for mode i

$$h_i(t) = \frac{1}{\omega_i\sqrt{1-\zeta_i^2}}\int_0 f(\tau)\exp[-\zeta\,\omega_i(t-\tau)]\sin[\omega_i\sqrt{1-\zeta_i^2}(t-\tau)]d\tau \tag{2}$$

in which ω_i and ζ_i are the modal frequency and damping ratio and $f(t)$ is the forcing function, and $\dot{h}_i(t)$ is the time derivative of $h_i(t)$. The coefficients a_i and c_i are real-valued, generalized effective participation factors given by

$$a_i = -2\mathrm{Re}[b_i s_i] \qquad c_i = -2\mathrm{Re}\,b_i \tag{3}$$

where s_i are roots of the system

$$s_i = \omega_i(-\zeta_i + \mathrm{i}\sqrt{1-\zeta_i}) \tag{4}$$

and

$$b_i = \frac{-(\mathbf{q}^T\mathbf{\Phi}_i)(\mathbf{\Phi}_i^T\mathbf{r})}{s_i m_i - s_i^{-1}k_i} \tag{5}$$

where m_i and k_i are the i-th modal mass and stiffness which can be obtained directly from the mode shapes, $\mathbf{\Phi}_i$, and frequencies of the system. In Eq. 5, $\mathbf{q}$ is a vector of constants such that $\mathbf{q}^T\mathbf{x}$ gives the response quantity of interest, where $\mathbf{x}$ is the vector of nodal displacements of the system. For example, if the relative displacement between nodes 1 and 2 is of interest, then $\mathbf{q} = [-1\ 1\ 0\ \cdots\ 0]^T$. The vector $\mathbf{r}$ is the influence vector of the forcing function, relating the points of application of the force to the degrees of freedom of the system. For systems excited by base motion, $-f(t)$ is the base acceleration and $\mathbf{r} = \mathbf{Mi}$, where $\mathbf{M}$ is the mass matrix of the system and $\mathbf{i}$ is the influence vector for base input.

The second term in the summation in Eq. 1 is due to the phase shift caused by the non-classical damping of the system and arises from the imaginary components of the mode shapes. For systems with classical damping, $c_i = 0$ and the above summation reduces to the well known modal superposition rule where a_i is the ordinary modal effective participation factor for such systems.

Taking the derivative of Eq. 1 and using the equality $\ddot{h}_i(t) = f(t) - 2\zeta_i\omega_i\dot{h}_i(t) - \omega_i^2 h_i(t)$, the following expression for the derivative response is obtained:

$$\dot{v}(t) = \sum_i [-\omega_i^2 c_i h_i(t) + (a_i - 2\zeta_i\omega_i c_i)\dot{h}_i(t) - c_i f(t)] \tag{6}$$

It has been shown (12) that the identity $\sum_i c_i \equiv 0$ is an intrinsic property of all linear systems. Therefore, the last term in the above summation can be dropped. Introducing the state vector $\mathbf{V} = [v(t) \quad \dot{v}(t)]^T$, Eqs. 1 and 6 can be written in matrix form

$$\mathbf{V} = \sum_i \mathbf{A}_i \mathbf{X}_i \tag{7}$$

where

$$\mathbf{A}_i = \begin{bmatrix} a_i & c_i \\ -\omega_i^2 c_i & a_i - 2\zeta_i\omega_i c_i \end{bmatrix} \qquad \mathbf{X}_i = \begin{Bmatrix} h_i(t) \\ \dot{h}_i(t) \end{Bmatrix} \tag{8}$$

The response cross-correlation matrix may now be written as

$$E[\mathbf{V}\mathbf{V}^T] = \sum_i \sum_j \mathbf{A}_i E[\mathbf{X}_i \mathbf{X}_j^T] \mathbf{A}_j^T \tag{9}$$

where

$$E[\mathbf{X}_i \mathbf{X}_j^T] = \begin{bmatrix} E[h_i(t_1)h_j(t_2)] & E[h_i(t_1)\dot{h}_j(t_2)] \\ E[\dot{h}_i(t_1)h_j(t_2)] & E[\dot{h}_i(t_1)\dot{h}_j(t_2)] \end{bmatrix} \tag{10}$$

The above matrix is the same used for nonstationary analysis of classically damped systems. The only difference is in matrix $\mathbf{A}_i$: For classically damped systems $\mathbf{A}_i = \mathrm{diag}\{a_i \quad a_i\}$. It follows that existing procedures for nonstationary response analysis of classically damped systems are directly applicable to non-classically damped systems, provided matrix $\mathbf{A}_i$ is properly modified. The procedure used in computing the cross-correlation matrix in Eq. 10 depends on the form of specification of the input excitation. If $f(t)$ is specified in the frequency domain through an evolutionary power spectral density, then a procedure such as in Ref. 7 is used, and if the input is specified in time domain by modulation, then a procedure such as in Refs. 14 or 5 is used. In particular, Ref. 5 contains closed form, time-domain solutions of the covariance matrix in Eq. 10 for piece-wise, linearly modulated white-noise inputs. These solutions were used in the present paper for the numerical example described in the following section.

To characterize the peak response of the system, the hazard function is used. Failure is defined to occur when the magnitude of the system response exceeds a barrier level a. Assuming non-homogeneous Poisson crossings, the reliability of the system is given by [2]

$$L(t) = \exp\left[-\int_0^t \alpha(\tau)\,d\tau\right] \tag{11}$$

where $L(t)$ = the probability of no barrier crossing (no failure) in the time interval $(0,t)$ and $\alpha(t)$ = the hazard function. Several solutions have been developed for the hazard function. Herein, the simplest form derived by Cramer and Leadbetter [3] is used:

$$\alpha(t) = \frac{1}{\pi}\sqrt{\frac{E[\dot{v}^2(t)]}{E[v^2(t)]}}\exp\left[-\frac{a^2}{2E[v^2(t)]}\right] \tag{12}$$

which is accurate for high barrier levels. The preceding expression neglects the contribution of the correlation between $v(t)$ and $\dot{v}(t)$, which is a valid approximation for the present application. For a specific t and exceedance probability P, the peak response fractile $a(t)$ is obtained by solving Eq. 11 with $L(t) = 1 - P$.

3. Numerical Investigation

To gain insight into the nonstationary response of secondary subsystems, the responses of a 7-degree-of-freedom, primary-secondary system to a class of nonstationary base excitations typical of short-duration earthquakes are examined. The excitation is modeled as a modulated white-noise process, where the modulating function is selected based on Type C envelope developed by Jennings, et al. [13] for short-duration earthquakes (see Fig. 1). The envelope has three distinct phases: An initial 2-second linear buildup, a constant, 2-second strong-motion phase ($D = 2$ in Fig. 1), and an 8-second tail with exponential decay rate 0.586. To investigate the effect of the duration of the seismic input on the response of the system, the above envelope is modified by varying the strong-motion duration, D. Specifically, D

$= 0.5$, 1.0, 2.0, 4.0, and 8.0 seconds are considered.

The system consists of the 4-degree-of-freedom secondary subsystem attached at two points to the 3-degree-of-freedom primary subsystem shown in Fig. 2. The properties of the individual subsystems and their modal frequencies are also given in Fig. 2. Observe that the modes of the two subsystems are closely tuned. Modal damping ratios are assumed to be 0.02 for the primary subsystem and 0.005 for the secondary subsystems. The responses considered are the relative horizontal displacement between the top two nodal points of the secondary subsystem and the displacement of the top mass of the primary subsystem relative to the base of the composite system.

The root-mean-square (RMS) responses of the two subsystems for the selected values of D are shown in Fig. 3. The vertical lines in this figure indicate the ends of the strong-motion phase of the ground motion in each case. The fundamental difference in the response of the two subsystems is that whereas the response of the primary subsystems sharply decays immediately after the strong-motion phase, the response of the secondary subsystem peaks long after termination of that phase. This is due to the beat phenomenon: The energy is transferred alternately between the two subsystems, and after the termination of the strong-motion phase energy transfers from the primary into the secondary subsystem resulting in the behavior discussed. The energy transfer can also be observed by comparing the response curves for the two subsystems. It is seen that where the RMS response of one subsystem is increasing, the RMS response of the other subsystem is decreasing.

In order to more clearly observe the effect of the beat phenomenon on the response of the secondary subsystem, the RMS responses are normalized by the maximum value occurring during the strong-motion phase. These are shown in Fig. 4, where it is observed that the ratio of the RMS's can be over 4 for very short duration earthquakes ($D = 0.5$ seconds).

In Fig. 5, the P-exceedance levels, $a_P(t)$ for $P = 0.05$, 0.10, and 0.20 are plotted as a function of time for the two subsystems and $D = 2.0$ seconds. This figure clearly indicates that whereas the peak response of the primary occurs shortly after the termination of the strong-motion phase, the peak response of the secondary occurs long after the termination.

4. Summary and Conclusions

It is shown that the response of tuned secondary subsystems to short-duration earthquakes is fundamentally different from that of ordinary structures. Specifically, the peak response of such subsystems may occur long after termination of the excitation in the free-vibration phase. This is due to the beat phenomenon occurring in tuned, interacting primary-secondary systems. A method for stochastic response analysis of general secondary systems is presented which accurately accounts for the important characteristics of such systems.

5. Acknowledgment

This research work is supported by the National Science Foundation under Grant No. CEE-8217800, which support is gratefully acknowledged.

References

1. American Society of Mechanical Engineers, *ASME Boiler and Pressure Vessel Code*, ANSI/ASME BPV-III-1-A Section III, Rules for Construction of Nuclear Power Plant Components, Division 1, Appendix N, July 1981.
2. R. B. Corotis, E. H. Vanmarcke, and C. A. Cornell, "First Passage of Nonstationary Random Processes," *Journal of the Engineering Mechanics Division*, vol. 98, no. EM2, pp. 401-414, April, 1972.
3. H. Cramer and M. R. Leadbetter, *Stationary and Related Stochastic Processes*, John Wiley and Sons, New York, N.Y., 1967.
4. A. Der Kiureghian, J. L. Sackman, and B. Nour-Omid, "Dynamic Analysis of Light Equipment in Structures: Response to Stochastic Input," *Journal of the Engineering Mechanics Division*, vol. 109, no. EM1, pp. 90-110, Feb., 1983.
5. D. A. Gasparini and A. DebChaudhury, "Dynamic Response to Nonstationary Nonwhite Excitation," *Journal of*

the Engineering Mechanics Division, vol. 106, no. EM6, December, 1980.

6. D. A. Gasparini, A. Shah, G. Tsiatas, S. L. Shien, and W.-J. Sun, "Random Vibration of Cascaded Secondary Systems," Case Institute of Technology, Dept. of Civil Engineering Research Report 83-1, January 1983.

7. J. K. Hammond, "On the Response of Single and Multidegree of Freedom Systems to Non-Stationary Random Excitations," *Journal of Sound and Vibration*, vol. 7, no. 3, pp. 393-416, 1968.

8. T. Igusa and A. Der Kiureghian, "Response Spectrum Method for Systems with Nonclassical Damping," in *Proceedings*, ASCE-EMD Specialty Conference, pp. 380-384, West Lafayette, Indiana, May 23-25, 1983.

9. T. Igusa and A. Der Kiureghian, "Non-Stationary Response of Secondary Systems," in *Proceedings*, ASCE-EMD Specialty Conference, pp. 1188-1191, Laramie, Wyoming, August 1-3, 1984.

10. T. Igusa and A. Der Kiureghian, "Dynamic Response of Multiply Supported MDOF Secondary Systems," *Journal of Engineering Mechanics*, vol. 111, no. 1, pp. 20-41, January 1985.

11. T. Igusa and A. Der Kiureghian, "Dynamic Characterization of Two-Degree-of-Freedom Equipment-Structure Systems," *Journal of Engineering Mechanics*, vol. 111, no. 1, pp. 1-19, January 1985.

12. T. Igusa, A. Der Kiureghian, and J.L. Sackman, "Modal Decomposition Method for Stationary Response of Nonclassically Damped Systems," *Earthquake Engineering and Structural Dynamics*, vol. 12, no. 1, pp. 121-136, 1984.

13. P. C. Jennings, G. W. Housner, and N. C. Tsai, *Simulated Earthquake Motions*, Earthquake Engineering Research Laboratory, California Institute of Technology, Pasadena, Calif., April 1968.

14. S. F. Masri, "Response of a Multi-Degree-of Freedom System to Nonstationary Random Excitation," *Journal of Applied Mechanics*, vol. 45, no. 3, pp. 649-656, September 1978.

15. J. L. Sackman and J. M. Kelly, "Seismic Analysis of Internal Equipment and Components in Structures," *Engineering Structures*, vol. 1, no. 4, pp. 179-190, July, 1979.

16. M.P. Singh and Y.K. Wen, "Nonstationary Seismic Response of Light Equipment," *Journal of Engineering Mechanics Division*, vol. 103, no. EM6, pp. 1035-1048, Dec., 1977.

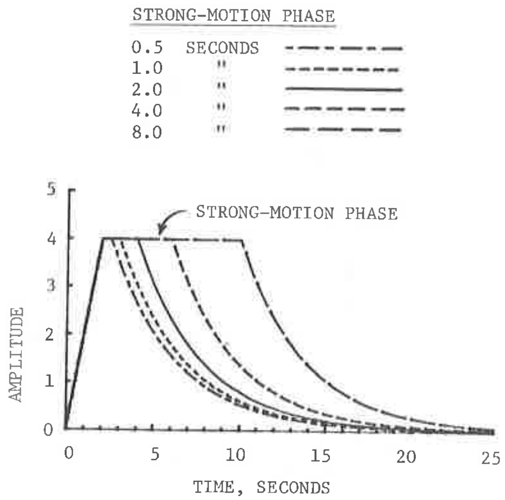

Figure 1. Modulating Function

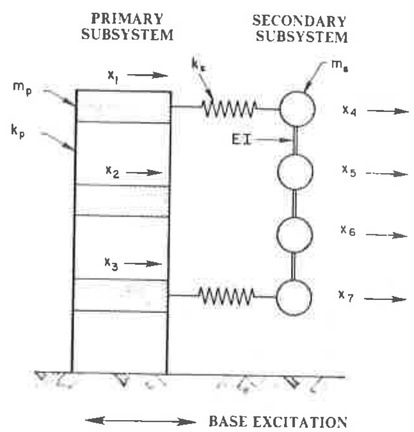

Figure 2. Example Primary-Secondary System

Table 1. Properties of Example Primary and Secondary Subsystems

Subsystem	Mode	Frequency (rad/sec)
Primary:	1	4.45
$k_p/m_p = 100$ rad^2/sec^2	2	12.50
$m_p = 10{,}000$ slugs	3	18.00
Secondary:	1	4.29
$k_s/m_s = 295$ rad^2/sec^2	2	9.76
$EI/L^3 m_s = 3.3$ rad^2/sec^2	3	17.80
$m_s = 200$ slugs	4	18.30

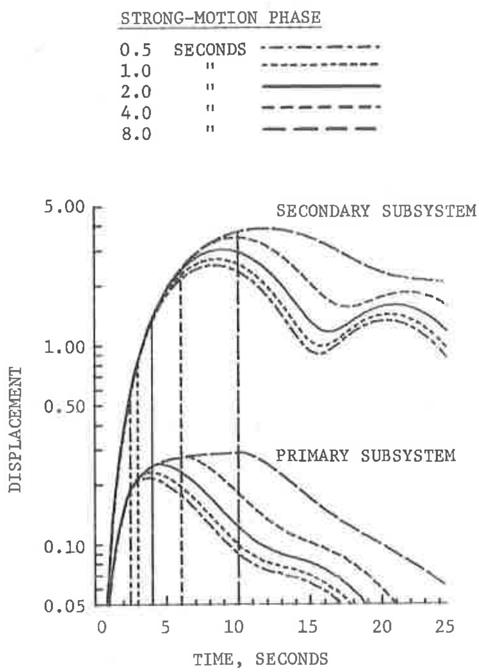

Figure 3. Root-Mean-Square Displacement Response

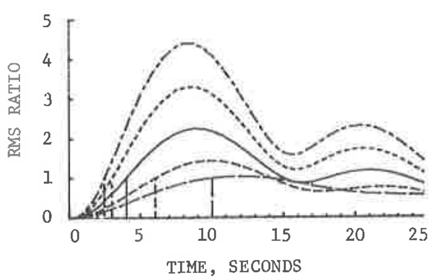

Figure 4. Normalized Root-Mean-Square Response

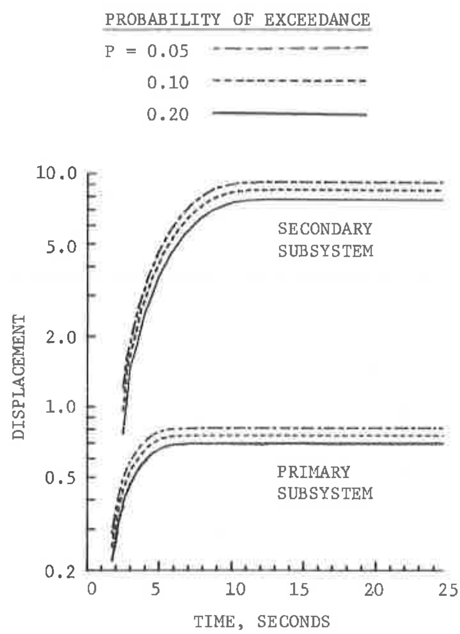

Figure 5. P-Exceedance Response Levels